

## Peripheral Stepwise Degradation of a Porphyrin J-Aggregate

Ilaria Occhiuto,<sup>†</sup> Giovanna De Luca,<sup>‡,§</sup> Mariachiara Trapani,<sup>†</sup> Luigi Monsù Scolaro,<sup>\*,†,⊥</sup> and Robert F. Pasternack<sup>||</sup><sup>†</sup>Dipartimento di Chimica Inorganica, Chimica Analitica e Chimica Fisica, Università di Messina, and CIRCMSB, viale Stagno d'Alcontres 31, 98166 Messina, Italy<sup>‡</sup>Dipartimento Farmaco-Chimico, Università di Messina, viale Annunziata, 98168 Messina, Italy<sup>§</sup>Istituto per i Materiali Compositi e Biomedici, CNR, P.le Tecchio 80, 80125 Naples, Italy<sup>⊥</sup>Istituto per lo Studio dei Materiali Nanostrutturati (ISMN), CNR, via dei Taurini 19, 00185 Rome, Italy<sup>||</sup>Department of Chemistry and Biochemistry, Swarthmore College, 500 College Avenue, Swarthmore, Pennsylvania 19081, United States

## S Supporting Information

**ABSTRACT:** For metalation of the acidic form of tetrakis(4-sulfonatophenyl)porphyrin (dianionic H<sub>4</sub>TPPS<sub>4</sub>) by Cu(II), the order of reagent mixing determines the rate and mechanism of CuTPPS<sub>4</sub> formation. When copper salts are added last, the kinetic profile is fit as a (pseudo)-first-order process. However, J-aggregates of the H<sub>4</sub>TPPS<sub>4</sub> porphyrin are rapidly formed at pH ~ 3 when Cu(II) salts are incorporated in solution prior to porphyrin addition. The subsequent porphyrin units metalation leads to the disassembling of these arrays via a pseudo-zero-order kinetic profile, suggesting an attack of the metal ion at the rims of the nanostructure.

J-aggregates (J-agg) formed via the self-assembly of porphyrins have attracted the attention of many researchers because of their remarkable structural, electronic, and chiral properties.<sup>1</sup> Much of this effort has been focused on water-soluble tetraanionic tetrakis(4-sulfonatophenyl)porphyrin (H<sub>2</sub>TPPS<sub>4</sub>). At acidic pH, the diacid H<sub>4</sub>TPPS<sub>4</sub> (pK<sub>a</sub> = 4.9)<sup>2</sup> is formed, which, in the presence of added salts or at high acid concentration, self-assembles to form nanostructures that are stabilized primarily by electrostatic interactions between the positive protonated core of the macrocycle and the negatively charged sulfonate groups of adjacent porphyrins. A series of studies have suggested the presence in solution of assemblies whose sizes span from the nano- to micrometer scale,<sup>3</sup> and recent investigations have provided evidence for the formation of porphyrin nanotubes.<sup>4</sup> Depending on the mixing protocol,<sup>5</sup> medium properties [pH, ionic strength (IS), etc.], and porphyrin concentration, an interesting “fractal-to-rod” transition of the aggregate mesostructure has also been reported.<sup>6</sup>

While at the mesoscopic scale the description of the aggregation kinetics can be analyzed in terms of current theories for colloidal systems,<sup>7</sup> at the nanoscale, the kinetics of J-agg supramolecular assembly are characterized by a sigmoidal profile with an initial lag period. These two phases correspond to an early nucleation stage, followed by a rapid growth of the aggregates.<sup>8</sup> An analysis of the kinetics has been provided by a complex model proposed by Pasternack et al.<sup>9</sup>

Detailed kinetic studies on the reverse reaction for J-agg, i.e., the disassembly process, are far less frequent.<sup>10</sup> However, such processes could prove important in a number of chemical/biochemical applications of J-agg assemblies in which such species serve, for example, as (unreactive) reservoirs of active monomers. Strategies for the stepwise freeing of these small, reactive molecules could be very useful, especially where time release is a factor. Here we describe the disassembly behavior of a J-agg nanostructure by interaction with Cu(II) ions. The selection of Cu(II) as the metal ion for this investigation is based on several factors: it inserts into porphyrins orders of magnitude more rapidly than other metal ions, forms a stable product [unlike Zn(II), whose complexes with porphyrins are labile at low pH], has little tendency to add axial ligands, and shows no (easily accessible) redox behavior.<sup>11</sup>

When a solution of CuSO<sub>4</sub> (0.3 M) is added to a preacidified solution of H<sub>4</sub>TPPS<sub>4</sub> (pH = 2.6), the B band of the starting monomeric porphyrin (434 nm) decreases with time, with a concomitant increase of the band at 412 nm due to the formation of CuTPPS<sub>4</sub> (Figure 1).<sup>12</sup> The corresponding kinetic traces (Figure 1, inset) can be fitted to monoexponential profiles and, as might be expected, the rate law is first-order in

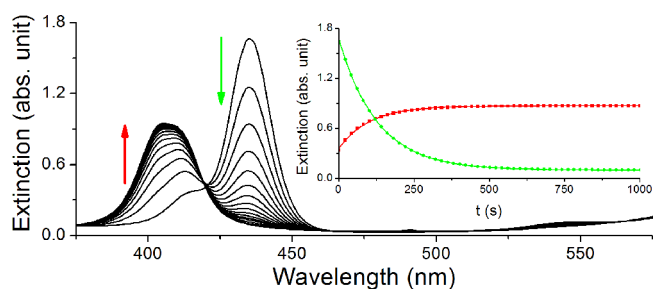


**Figure 1.** UV/vis spectral changes and kinetic traces (inset; green, 434 nm; red, 412 nm) for Cu(II) insertion in H<sub>4</sub>TPPS<sub>4</sub>, adding the porphyrin as the “first reagent”. Experimental conditions: [CuSO<sub>4</sub>] = 0.3 M.  $k_{\text{obs}} = (7.81 \pm 0.01) \times 10^{-3} \text{ s}^{-1}$ , leading to a second-order rate constant  $k_2 = (2.6 \pm 0.1) \times 10^{-2} \text{ M}^{-1} \text{ s}^{-1}$ .

Received: July 19, 2012

Published: September 13, 2012

both porphyrin and Cu(II) concentrations.<sup>11</sup> Values obtained for the rate constants are in agreement at the two wavelengths [ $k_2 = (2.6 \pm 0.1) \times 10^{-2} \text{ M}^{-1} \text{ s}^{-1}$ ], and they are consistently lower than those reported in the literature for metalation of the  $\text{H}_2\text{TPPS}_4$  free base because of the pH being lower.<sup>11</sup>

However, when the porphyrin is added as the final reagent to a premixed solution containing both acid and Cu(II), a much more complicated pattern of behavior is observed. Figure 2

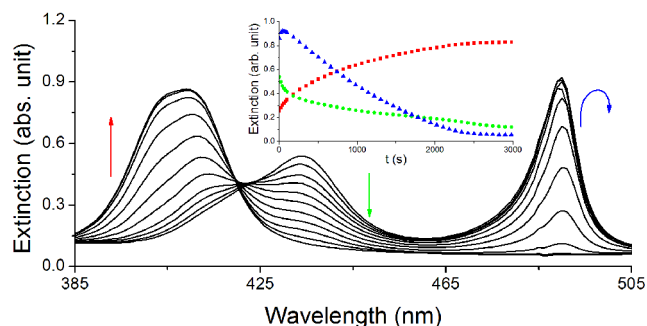


**Figure 2.** UV/vis spectral changes and kinetic traces (inset) for Cu(II) insertion in  $\text{H}_4\text{TPPS}_4$ , adding the porphyrin as the “last reagent”. The arrows mark the decreasing  $\text{H}_4\text{TPPS}_4$  (green), the increasing  $\text{CuTPPS}_4$  (red), and the evolution of the transient J-agg (blue). Inset:  $\lambda = 434 \text{ nm}$  (green),  $412 \text{ nm}$  (red), and  $490 \text{ nm}$  (blue). Experimental conditions:  $[\text{CuSO}_4] = 0.3 \text{ M}$ .

shows that the B band of the diacid species ( $434 \text{ nm}$ ) decreases at the beginning of the process, accompanied by an increase of a new band at  $490 \text{ nm}$  that is attributable to J-agg formation.<sup>13</sup> After this fast initial step, the J-agg band decreases, accompanied by a further intensity reduction of the band at  $434 \text{ nm}$  and a progressive increase of absorption at  $412 \text{ nm}$  ( $\text{CuTPPS}_4$  Soret absorption maximum). Cu(II) plays a dual role in this process: it screens the electrostatic repulsion among porphyrins, favoring their aggregation, and it serves as a metallating reagent, complexing the porphyrin core and causing the disassembly of the nanostructure. The complex time evolution of this system is shown in Figure 2, inset, with a near-linear profile for the extinction decay at  $490 \text{ nm}$  corresponding to pseudo-zero-order kinetics for the disappearance of the J-agg.

To investigate the effect of the Cu(II) concentration on the rate of this assembly–disassembly process, we have performed a series of kinetic experiments starting from  $[\text{CuSO}_4] = 0.05 \text{ M}$ , which ensures the formation of a detectable amount of J-agg in the reaction mixture. When the concentration is increased up to  $[\text{CuSO}_4] = 0.3 \text{ M}$ , both the rates of  $\text{H}_4\text{TPPS}_4$  self-assembly and subsequent metalation increase. Above this concentration, a further increase up to  $[\text{CuSO}_4] = 0.8 \text{ M}$  causes a decrease in the overall rate for metalation (Figure S12 in the Supporting Information). The bell-shaped dependence of the metalation rates on the copper(II) ion concentration is a consequence of competitive phenomena: on the one hand, stabilization of the J-agg with increasing IS; on the other hand, a parallel increase in the metalation rate. To disentangle these two factors, we measured the metalation rates on preformed J-agg versus the Cu(II) ion concentration at an IS maintained at  $2 \text{ M}$  by complementing  $\text{CuSO}_4$  with the appropriate amount of  $\text{Na}_2\text{SO}_4$  (Figure 3). Under these conditions, we observe that (i) J-agg are stabilized and the metalation process is slower with respect to the experiments conducted with variable salt concentration at lower IS and (ii) there is a linear dependence

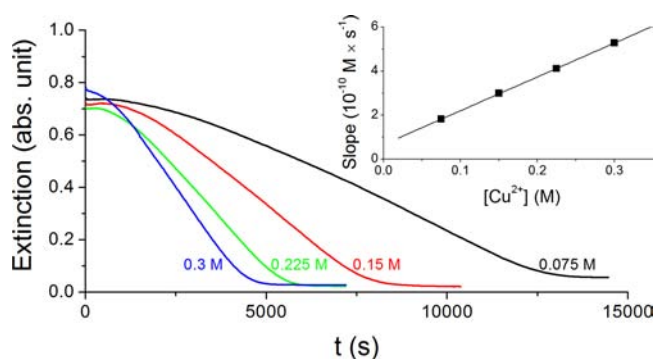
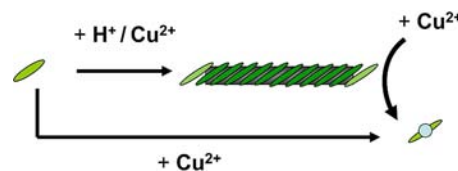


**Figure 3.** Extinction changes at  $490 \text{ nm}$  for the Cu(II) insertion in preformed J-agg according to protocol (iii) as a function of the added  $\text{CuSO}_4$ . Inset: values of the slopes obtained from a linear fit of the extinction changes at  $490 \text{ nm}$  versus Cu(II) ion concentration. Black line: slope =  $(1.53 \pm 0.01) \times 10^{-9} \text{ s}^{-1}$ ; intercept =  $(6.72 \pm 0.2) \times 10^{-11} \text{ M s}^{-1}$ . Experimental conditions: labels indicate  $[\text{CuSO}_4]$ ; IS =  $2 \text{ M}$  by the addition of  $\text{Na}_2\text{SO}_4$ .

of the metalation rates on Cu(II) concentration. Furthermore, we note a small nonzero intercept at  $[\text{Cu}^{2+}] = 0 \text{ M}$ , suggesting a pathway for metalation that is independent of Cu(II) concentration. This effect is currently under investigation, but we speculate that it might be ascribed to end molecules dissociating from the aggregate and being rapidly scavenged by Cu(II) ions.

The experimental kinetic evidence suggests a mechanism for the assembly and disassembly processes under investigation, as shown in Scheme 1. The diacid porphyrin units self-organize

#### Scheme 1. Simplified Mechanistic Sketch for the Assembly and Subsequent Disassembly Processes of $\text{H}_4\text{TPPS}_4$ Mediated by Cu(II) Ions in Acidic Aqueous Solutions



nanoarrays (“seeds”), and this process is fostered under acidic conditions and/or by an increase of the IS, in our case by the addition of  $\text{CuSO}_4$ . However, the initial mixing protocol determines the actual transition pathway and the role of J-agg.

When the acidified porphyrin is *prediluted* in an acidic solution, the addition of Cu(II) salt as the “last reagent” does not promote aggregation but leads directly to formation of the metalloporphyrin. On the other hand, when a  $\text{H}_2\text{TPPS}_4$  stock solution is added to a mixture of acid and salt, the higher local concentration of the porphyrin triggers the nucleation process and J-agg are formed.<sup>5</sup> The extent of aggregation increases with the  $\text{CuSO}_4$  concentration because the resulting aggregates are stabilized by the higher IS. Copper(II) insertion into the macrocycle can occur through direct metalation of the monomeric  $\text{H}_4\text{TPPS}_4$  or through attack on the J-agg, the two predominant porphyrin species in solution. Given the putative structure of the nanoaggregates,<sup>4</sup> it is not unreasonable to assume a lowered reactivity or even nonreactivity of the porphyrins embedded in the inner part of the structure, similar to other nanoassemblies.<sup>10c</sup> The central core of the inner porphyrin units is both protonated and involved in hydrogen

bonding with sulfonate groups that sterically hinder attack above and below the porphyrin plane. In contrast, the porphyrins at the ends of the nanostructure are exposed and are, therefore, expected to be more reactive. These are the most likely sites for Cu(II) attack. Consequently, J-aggs are disassembled by metalation, maintaining constant their mean concentration even while reducing their size, thus explaining the observed pseudo-zero-order kinetics; i.e., the J-aggs are serving as reservoirs of porphyrin reactive units. Indeed, this hypothesis is supported by a comparison of the kinetic traces observed for the same kinetic run using UV/vis extinction and resonance light scattering (RLS; Figure 4). The steeper slope

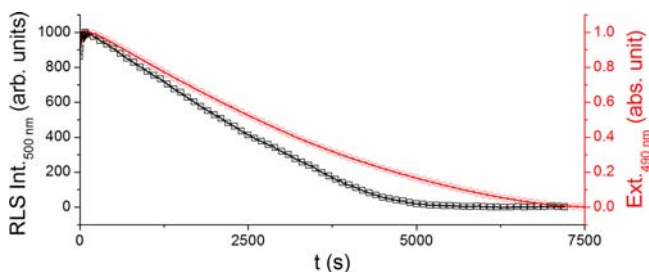


**Figure 4.** Normalized kinetic traces monitored by RLS at 500 nm (black) and UV/vis extinction at 490 nm (left) for Cu(II) insertion in the porphyrin  $H_4TPPS_4$ . Experimental conditions:  $[CuSO_4] = 0.1 M$ ; porphyrin added last.

for the RLS results reflects the greater sensitivity of this method to the aggregate size.<sup>14</sup> We exclude a mechanism involving a direct attack on porphyrins deeply embedded within the nanostructures because that would lead to fragmentation of the nanoassemblies, formation of additional reactive ends, and acceleration of the rates according to an autocatalytic scheme.<sup>10c</sup> The bell-shaped dependence of the rates on the Cu(II) ion reflects a competitive stabilization of the J-aggs on increasing the IS and a concomitant increase in the metalation rate.

In spite of the large amount of data on the reactivity of monomeric porphyrins toward metalation reactions, very few studies have been reported on their aggregated species. J-aggregates are attracting increasing interest by the scientific community for many different applications, and therefore a knowledge of their kinetic behavior is very important to the design of supramolecular devices. The results reported here provide an example of the complexity of these systems, involving kinetically and thermodynamically coupled supramolecular assembly processes.

## ■ ASSOCIATED CONTENT

### 📄 Supporting Information

Experimental methods and kinetic data for the formation of J-aggs in the absence and presence of Cu(II) sulfate. This material is available free of charge via the Internet at <http://pubs.acs.org>.

## ■ AUTHOR INFORMATION

### Corresponding Author

\*E-mail: [lmonsu@unime.it](mailto:lmonsu@unime.it).

### Notes

The authors declare no competing financial interest.

## ■ ACKNOWLEDGMENTS

The authors thank Gaetano Irrera (ISMN-CNR) and Salvatore Todaro (UniME) for technical assistance and useful discussions. This work was supported by MIUR-PRIN 2008A9C4HZ.

## ■ REFERENCES

- (1) (a) Würthner, F.; Kaiser, T. E.; Saha-Möller, C. R. *Angew. Chem., Int. Ed.* **2011**, *50*, 3376–3410. (b) Kitagawa, Y.; Segawa, H.; Ishii, K. *Angew. Chem., Int. Ed.* **2011**, *50*, 9133–9136. (c) D'Urso, A.; Randazzo, R.; Lo Taro, L.; Purrello, R. *Angew. Chem., Int. Ed.* **2010**, *49*, 108–112. (d) Collini, E.; Ferrante, C.; Bozio, R. *J. Phys. Chem. C* **2007**, *111*, 18636–18645. (e) Kobayashi, T.; Kano, H. *Nonlinear Opt., Quantum Opt.* **2004**, *31*, 115–135. (f) Ribó, J. M.; Crusats, J.; Sagues, F.; Claret, J.; Rubires, R. *Science* **2001**, *292*, 2063–2066.
- (2) Kalyanasundaram, K. *Photochemistry of Polypyridine and Porphyrin Complexes*; Academic Press: London, 1992.
- (3) (a) Rotomskis, R.; Augulis, R.; Snitka, V.; Valiokas, R.; Liedberg, B. *J. Phys. Chem. B* **2004**, *108*, 2833–2838. (b) Schwab, A. D.; Smith, D. E.; Rich, C. S.; Young, E. R.; Smith, W. F.; de Paula, J. C. *J. Phys. Chem. B* **2003**, *107*, 11339–11345. (c) Collings, P. J.; Gibbs, E. J.; Starr, T. E.; Vafek, O.; Yee, C.; Pomerance, L. A.; Pasternack, R. F. *J. Phys. Chem. B* **1999**, *103*, 8474–8481. (d) Ribó, J. M.; Crusats, J.; Farrera, J. A.; Valero, M. L. *J. Chem. Soc., Chem. Commun.* **1994**, 681–682. (e) Akins, D. L.; Zhu, H. R.; Guo, C. *J. Phys. Chem.* **1994**, *98*, 3612–3618.
- (4) (a) Rich, C. C.; McHale, J. L. *Phys. Chem. Chem. Phys.* **2012**, *14*, 2362–2374. (b) Hollingsworth, J. V.; Richard, A. J.; Vicente, M. G. H.; Russo, P. S. *Biomacromolecules* **2012**, *13*, 60–72. (c) Friesen, B. A.; Wiggins, B.; McHale, J. L.; Mazur, U.; Hipps, K. W. *J. Am. Chem. Soc.* **2010**, *132*, 8554–8555. (d) Vlaming, S. M.; Augulis, R.; Stuart, M. C. A.; Knoester, J.; van Loosdrecht, P. H. M. *J. Phys. Chem. B* **2009**, *113*, 2273–2283. (e) Friesen, B. A.; Nishida, K. R. A.; McHale, J. L.; Mazur, U. *J. Phys. Chem. C* **2009**, *113*, 1709–1718. (f) Gandini, S. C. M.; Gelamo, E. L.; Itri, R.; Tabak, M. *Biophys. J.* **2003**, *85*, 1259–1268.
- (5) Castriciano, M. A.; Romeo, A.; Villari, V.; Micali, N.; Scolaro, L. M. *J. Phys. Chem. B* **2003**, *107*, 8765–8771.
- (6) Micali, N.; Villari, V.; Castriciano, M. A.; Romeo, A.; Scolaro, L. M. *J. Phys. Chem. B* **2006**, *110*, 8289–8295.
- (7) Micali, N.; Mallamace, F.; Romeo, A.; Purrello, R.; Scolaro, L. M. *J. Phys. Chem. B* **2000**, *104*, 5897–5904.
- (8) The kinetic profiles are strongly dependent on the reagent mixing order: adding the porphyrin as the last reagent leads to a fast nucleation with a concomitant substantial reduction or disappearance of the lag period.<sup>7</sup>
- (9) (a) Pasternack, R. F.; Fleming, C.; Herring, S.; Collings, P. J.; de Paula, J.; DeCastro, G.; Gibbs, E. J. *Biophys. J.* **2000**, *79*, 550–560. (b) Pasternack, R. F.; Gibbs, E. J.; Collings, P. J.; de Paula, J. C.; Turzo, L. C.; Terracina, A. *J. Am. Chem. Soc.* **1998**, *120*, 5873–5878.
- (10) (a) Watanabe, K.; Kano, K. *Bioconjugate Chem.* **2010**, *21*, 2332–2338. (b) Kano, K.; Watanabe, K.; Ishida, Y. *J. Phys. Chem. B* **2008**, *112*, 14402–14408. (c) Pasternack, R. F.; Gibbs, E. J.; Bruzewicz, D.; Stewart, D.; Engstrom, K. S. *J. Am. Chem. Soc.* **2002**, *124*, 3533–3539.
- (11) Schneider, V. *Struct. Bonding (Berlin)* **1975**, *23*, 123–166.
- (12) The band at 412 nm corresponding to the  $CuTPPS_4$  metal porphyrin is accompanied by a second band at 405 nm, which could be ascribed to a dimer of this compound. The relative amounts of the two species change as a function of the salt concentration because the equilibrium is forced toward the dimer at higher IS. See: Kemnitz, K.; Sakaguchi, T. *Chem. Phys. Lett.* **1992**, *196*, 497–503.
- (13) This process can be isolated by forming J-aggs through the use of sodium rather than Cu(II) sulfate, revealing this process to be much faster ( $t_{1/2} < 3$  s; see Figure S11 in the Supporting Information) than Cu(II) metalation ( $t_{1/2} \sim 100$  s; see Figure 1, inset).
- (14) Parkash, J.; Robblee, J. H.; Agnew, J.; Gibbs, E.; Collings, P.; Pasternack, R. F.; de Paula, J. C. *Biophys. J.* **1998**, *74*, 2089–2099.